

Conformational Nonequilibrium Enzyme Kinetics: Generalized Michaelis-Menten Equation

Jianlan Wu,* D. Evan Piephoff, and Jianshu Cao†

Department of Chemistry, Massachusetts Institute of Technology, Cambridge, Massachusetts 02139, USA

In a conformational nonequilibrium steady state (cNESS), enzyme turnover is modulated by the underlying conformational dynamics. Based on a discrete kinetic network model, we use the integrated population flux balance method to derive the cNESS turnover rate for a conformation-modulated enzymatic reaction. The traditional Michaelis-Menten (MM) rate equation is extended to a generalized form, which includes non-MM corrections induced by conformational population currents within combined cyclic kinetic loops. When conformational detailed balance is satisfied, the turnover rate reduces to the MM functional form, explaining its general validity for many enzymatic systems. In addition, a one-to-one correspondence is shown between non-MM terms and combined cyclic loops with unbalanced conformational currents, revealing a unique relation between the cNESS turnover rate and the underlying network topology. Cooperativity resulting from nonequilibrium conformational dynamics, referred to as ‘kinetic cooperativity,’ has been observed in enzymatic reactions, and we provide a novel, rigorous approach for predicting and characterizing such behavior, which includes positive and negative cooperativity as well as substrate inhibition. Using reduced parameters from the generalized MM equation, we construct phase diagrams of the non-MM enzyme kinetics and analyze cooperative behavior for single- and multi-loop models. Our generalized MM equation affords a systematic approach for exploring cNESS enzyme kinetics.

Introduction.—Conformational dynamics is essential for understanding the biological functions of enzymes. For decades, the framework of enzymatic reactions has been the traditional Michaelis-Menten (MM) mechanism [1], where enzyme-substrate binding initializes an irreversible catalytic reaction to form a product. The average turnover rate v in a steady state (SS) follows a hyperbolic dependence on the substrate concentration $[S]$, $v = k_2[S]/(K_M + [S])$, where the catalytic rate k_2 and the Michaelis constant K_M characterize this enzymatic chain reaction. In contrast to the single-conformation assumption for the traditional MM mechanism, recent single-molecule experiments [2–4] have revealed the existence of multiple enzymatic conformations, spanning a broad range of lifetime scales from milliseconds to hours. Conformational dynamics, including hopping between different conformations and thermal fluctuations around a single-conformation potential well, must be incorporated into enzymatic reaction models for a quantitative study [3, 5–18]. Slow conformational dynamics modulate the enzymatic reaction and allow the enzyme to exist in a conformational nonequilibrium steady state (cNESS), permitting complex deviations from MM kinetics (the hyperbolic $[S]$ dependence for v). However, experimental and theoretical studies have shown MM kinetics to be valid in the presence of slow conformational dynamics under certain conditions, although k_2 and K_M become averaged over conformations [3, 10, 15]. Is there a unifying theme governing this surprising behavior?

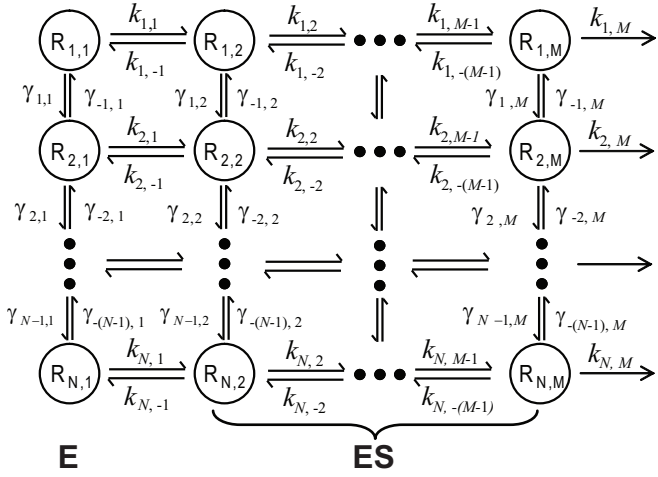
Non-MM enzyme kinetics have been characterized by cooperativity for many years [5, 6, 19]. For allosteric enzymes with multiple binding sites, the binding event at one site can alter the reaction activity at another site, accelerating (decelerating) the turnover rate and resulting

in positive (negative) cooperativity [19]. Another common deviation from MM kinetics is substrate inhibition, where the turnover rate reaches its maximum value at a finite substrate concentration and then decreases at high substrate concentrations [19]. For a monomeric enzyme, the above non-MM kinetic behavior, referred to – in this case – as ‘kinetic cooperativity’ [19], can be achieved by a completely different mechanism: nonequilibrium conformational dynamics [5, 6, 11–15]. Can we characterize and predict this interesting behavior in a cNESS?

Recently, theoretical efforts have been applied to study conformation-modulated enzyme kinetics by including dynamics along a conformational coordinate. On the basis of the usual rate approach, some previous work has demonstrated certain non-MM kinetics under specific conditions [10, 12–14, 16]. Based on an alternative integrated population flux balance method, non-MM kinetics were linked to a nonzero conformational population current, i.e., broken conformational detailed balance, in a two-conformation model, and a general MM expression was speculated [15]. However, a generalized theory to systematically analyze cNESS enzyme kinetics is still needed. In this Letter, we focus on a monomeric enzyme and apply the integrated flux balance method to derive a generalized form for the turnover rate, which includes non-MM corrections. We show that when conformational detailed balance is satisfied, MM kinetics hold, explaining their general validity. In addition, the deviations from MM kinetics are analyzed with reduced parameters from the generalized form of v . For an extended version of our derivation, we refer readers to Ref. [20].

Model and flux balance method.—To describe the generalized conformation-modulated reaction catalyzed by a monomeric enzyme, we introduce a discrete kinetic

a) kinetic network



b) flux network

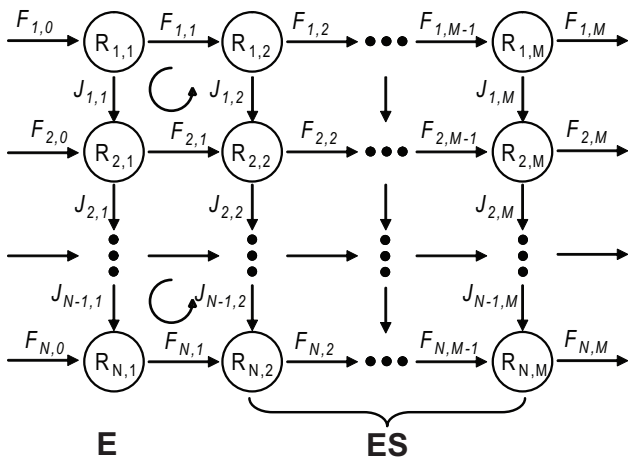


Figure 1. (a) Generalized kinetic network scheme for a conformation-modulated enzymatic reaction. (b) Flux network corresponding to (a) (see text for details).

network model, which is illustrated in Fig. 1(a). This $N \times M$ network consists of a vertical conformation coordinate ($1 \leq i \leq N$) and a horizontal reaction coordinate ($1 \leq j \leq M$). For the reaction state index, $j = 1$ denotes the initial substrate-unbound enzymatic state (E), whereas $j \geq 2$ denotes intermediate substrate-bound enzymatic states (ES) [3, 14, 15, 21, 22]. Without product states, our network corresponds to a dissipative system. For an arbitrary site $R_{i,j}$, the reaction rates for the forward ($R_{i,j} \rightarrow R_{i,j+1}$) and backward ($R_{i,j} \rightarrow R_{i,j-1}$) directions are given by $k_{i,j}$ and $k_{i,-(j-1)}$, respectively. The rate for enzyme-substrate binding, the only step in our model dependent upon substrate concentration $[S]$, depends linearly on $[S]$ as $k_{i,1} = k_{i,1}^0 [S]$ for binding rate constant $k_{i,1}^0$, with $[S]$ maintained constant in most enzymatic experiments. The

conformational dynamics are treated via a kinetic rate approach, with the interconversion (hopping or diffusion) rates for $R_{i,j} \rightarrow R_{i+1,j}$ and $R_{i,j} \rightarrow R_{i-1,j}$ given by $\gamma_{i,j}$ and $\gamma_{-(i-1),j}$, respectively. We note that local detailed balance results in the constraint $k_{i,j}\gamma_{-(i-1),j}/(k_{i,-(j-1)}\gamma_{i,j}) = k_{i+1,j}\gamma_{-(i-1),j+1}/(k_{i+1,-(j-1)}\gamma_{i,j+1})$ for $j \leq M-1$. However, for the purposes of our kinetic analysis, it is unnecessary to impose this relation, as our principal results hold, irrespective of whether it is satisfied. The rate equation for site $R_{i,j}$ is written as

$$\frac{d}{dt}P_{i,j}(t) = \sum_{i'=1}^N \gamma_{i,i';j} P_{i',j}(t) + \sum_{j'=1}^M k_{j,j';i} P_{i,j'}(t), \quad (1)$$

where $P_{i,j}(t)$ is the probability of an enzyme in site $R_{i,j}$ at time t , i.e., the survival probability for the site. Here, $\gamma_{i,i';j} = \gamma_{i-1,j}\delta_{i',i-1} + \gamma_{-i,j}\delta_{i',i+1} - [\gamma_{i,j} + \gamma_{-(i-1),j}]\delta_{i',i}$ denotes the interconversion rates in the j -th reaction state and $k_{j,j';i} = k_{i,j-1}\delta_{j',j-1} + \gamma_{i,-j}\delta_{j',j+1} - [k_{i,j} + k_{i,-(j-1)}]\delta_{j',j}$ denotes the reaction rates for the i -th conformation.

Within the framework of a dissipative enzymatic network, the average turnover rate v is equivalent to the inverse of the mean first passage time (MFPT) $\langle t \rangle$. Using the residence time $\tau_{i,j} = \int_0^\infty P_{i,j}(t)dt$ at each site $R_{i,j}$, we can express the MFPT in the $N \times M$ network as a summation of $\tau_{i,j}$, i.e., $\langle t \rangle = \sum_{i,j} \tau_{i,j}$. Instead of inverting the transition matrix [3], we evaluate $\tau_{i,j}$ by inspecting integrated population fluxes [15], which correspond to steady-state fluxes normalized by v , and these will be shown to directly reflect conformational nonequilibrium. Along the horizontal reaction coordinate, the integrated flux for $R_{i,j} \rightarrow R_{i,j+1}$ is given by $F_{i,j} = k_{i,j}\tau_{i,j} - k_{i,-(j-1)}\tau_{i,j+1}$. Along the vertical conformation coordinate, the integrated flux for $R_{i,j} \rightarrow R_{i+1,j}$ is given by $J_{i,j} = \gamma_{i,j}\tau_{i,j} - \gamma_{-(i-1),j}\tau_{i+1,j}$. In addition, we need to specify the initial condition $P_{i,j}(t=0)$ for calculating $\langle t \rangle$. For a monomeric enzyme, each turnover event begins with the substrate-unbound state, and $P_{i,1}(t=0)$ defines the initial flux $F_{i,0}$. With the definition of $\{F_{i,j}, J_{i,j}\}$, we map the original kinetic network to a flux network as shown in Fig. 1(b). For each site $R_{i,j}$, the rate equation in Eq. (1) is replaced by a flux balance relation,

$$F_{i,j-1} + J_{i-1,j} = F_{i,j} + J_{i,j} \quad (2)$$

which is generalized to the population conservation law: *the total input integrated population flux must equal the total output integrated population flux*. This conservation law can be extended to complex first-order kinetic structures including the $N \times M$ network. The flux balance method thus provides a simple means of calculating the MFPT.

Generalized Michaelis-Menten equation.—To evaluate the MFPT, we begin with the final reaction state ($j =$

M) and propagate all the fluxes back to the initial reaction state ($j = 1$) based on Eq. (2). For each site $R_{i,j}$, the physical nature of the first-order kinetics determines that all three variables, $\tau_{i,j}$, $J_{i,j}$ and $F_{i,j}$, are linear combinations of terminal fluxes $F_{i,j=M}$. The first two variables are formally written as $\tau_{i,j} = \sum_{i'=1}^N a_{i,j,i'} F_{i',M}$ and $J_{i,j} = \sum_{i'} c_{i,j,i'} F_{i',M}$, where $a_{i,j,i'}$ and $c_{i,j,i'}$ are coefficients depending on rate constants $\{k, \gamma\}$. For example, the coefficients for the final reaction state are $a_{i,M,i'} = 1/k_{i,M} \delta_{i',i}$ and $c_{i,M,i'} = \gamma_{i,M}/k_{i,M} \delta_{i',i} - \gamma_{-i,M}/k_{i+1,M} \delta_{i',i+1}$. Because of the direction of our reversed flux propagation, only the coefficients for the initial reaction state are $[S]$ dependent, and they can be explicitly written as $a_{i,1,i'} = b_{i,i'}/[S]$ and $c_{i,1,i'} = d_{i,i'}/[S]$. The substrate-unbound ($E_i = R_{i,1}$) and substrate-bound ($ES_i = \sum_{j=2}^M R_{i,j}$) states are distinguished by the different $[S]$ dependence of the coefficients. The MFPT is thus given by

$$\langle t \rangle = \sum_{i'=1}^N \left[\frac{\sum_{i=1}^N b_{i,i'}}{[S]} + \sum_{i=1}^N \sum_{j=2}^M a_{i,j,i'} \right] F_{i',M}. \quad (3)$$

The essential part of our derivation is then to solve for the terminal fluxes $F_{i,M}$. The SS condition can be interpreted as follows: after each product release, the enzyme returns to the same conformation for the next turnover reaction, i.e., $F_{i,M} = F_{i,0}$ [7]. Applying the population conservation law to each horizontal chain reaction with a single conformation and considering the boundary condition at conformations $i = 1$ and N , we express the SS condition as a flux constraint, $J_{i,E} + J_{i,ES} = 0$ for $i = 1, 2, \dots, N-1$, where $J_{i,E} = J_{i,1}$ and $J_{i,ES} = \sum_{j=2}^M J_{i,j}$. For each combined cyclic loop $E_i \rightarrow E_{i+1} \rightarrow ES_{i+1} \rightarrow ES_i \rightarrow E_i$, there may exist a stabilized nonequilibrium conformational population current [see Fig. 1(b)], with $J_{i,E}$ representing this steady-state current normalized by v . However, under certain circumstances, $J_{i,E}$ can vanish, and the SS condition is further simplified to $J_{i,ES} = 0$. We note that satisfaction of the aforementioned constraint resulting from local detailed balance still permits nonzero $J_{i,E}$. In general, we assume that there exist N_c ($\leq N-1$) nonzero conformational currents and $(N-1-N_c)$ zero ones. In addition to these $(N-1)$ current conditions, the normalization condition $\sum_{i=1}^N F_{i,0} = 1$ is needed for fully determining the initial fluxes (due to $F_{i,0} = F_{i,M}$). As a result, we derive an N -equation array for $F_{i,0}$,

$$\mathbf{U} \cdot \mathbf{F} = \begin{bmatrix} 1 & 1 & \dots \\ C_{1,1} + \left(\frac{d_{1,1}}{[S]} \right) & C_{1,2} + \left(\frac{d_{1,2}}{[S]} \right) & \dots \\ C_{2,1} + \left(\frac{d_{2,1}}{[S]} \right) & C_{2,2} + \left(\frac{d_{2,2}}{[S]} \right) & \dots \\ \vdots & \vdots & \vdots \end{bmatrix} \cdot \begin{bmatrix} F_{1,0} \\ F_{2,0} \\ \vdots \end{bmatrix} = \begin{bmatrix} 1 \\ 0 \\ \vdots \end{bmatrix}, \quad (4)$$

with $C_{i,i'} = \sum_{j=2}^M c_{i,j,i'}$. Notice that for the $(i+1)$ -th row of matrix \mathbf{U} in Eq. (4), $d_{i,i'}/[S]$ only exists when $J_{i,E} \neq 0$, and N_c rows are $[S]$ dependent for this matrix. We solve for the initial fluxes by the matrix inversion $F_{i,0} = [\mathbf{U}^{-1}]_{i,1}$. After a tedious but straightforward derivation, $F_{i,0}$ is written as

$$F_{i,0}([S]) = f_{i,0} + \sum_{n=1}^{N_c} f_{i,n}/([S] + s_n), \quad (5)$$

where each s_n is assumed to be distinct, and constraints hold for $\sum_i f_{i,0} = 1$ and $\sum_i f_{i,n} = 0$ for $n \geq 1$.

Substituting Eq. (5) into Eq. (3), we obtain the key result of this Letter: the cNESS turnover rate for the $N \times M$ network with N_c unbalanced conformational currents is given by a generalized Michaelis-Menten equation,

$$v = \left[A_0 + \frac{B_0}{[S]} + \sum_{n=1}^{N_c} \frac{B_n}{[S] + s_n} \right]^{-1}, \quad (6)$$

where the reduced parameters are $A_0 = \langle 1/k_2^{\text{eff}} \rangle_{[S] \rightarrow \infty}$, $B_0 = \langle K_M^{\text{eff}}/k_2^{\text{eff}} \rangle_{[S]=0}$, and $B_n = \sum_i [1/k_{i,2}^{\text{eff}} - K_{i,M}^{\text{eff}}/(k_{i,2}^{\text{eff}} s_n)] f_{i,n}$. For each conformational channel, we introduce an effective catalytic rate $k_{i,2}^{\text{eff}} = (\sum_{i'=1}^N \sum_{j=2}^M a_{i',j,i})^{-1}$ and an effective Michaelis constant $K_{i,M}^{\text{eff}} = k_{i,2}^{\text{eff}} \sum_{i'} b_{i',i}$, which describe the kinetics within that channel in the decomposed representation of the scheme, wherein the N two-state chain reactions are effectively independent, each with probability $F_{i,0}$. The conformational average is defined as $\langle x \rangle_{[S]} = \sum_i x_i F_{i,0}([S])$ for a conformation-dependent variable x_i . In the right hand side of Eq. (6), the first two terms retain the traditional MM form, whereas the remaining N_c terms introduce non-MM rate behavior, with a 1:1 correspondence between non-MM terms and combined cyclic loops with nonzero conformational currents. Our derivations clearly show that these non-MM terms are induced by the $[S]$ -dependent conformational distribution \mathbf{F} resulting from nonequilibrium conformational currents. Therefore, MM kinetics are valid when conformational detailed balance is satisfied, where all B_n vanish due to $F_{i,0} = f_{i,0}$.

Single-loop kinetics.—With nonzero conformational currents, the enzyme kinetics are expected to exhibit cooperative non-MM behavior. As a demonstration, the single-loop model with only one current $J_{1,E}$ and one non-MM term $B_1/([S] + s_1)$ is first considered. With other parameters fixed, we calculate turnover rates v for the three values of B_1 in Fig. 2(a). For the two turnover rates monotonically increasing with $[S]$ ($B_1 = -1$ and 2), we fit them with the Hill equation, $v/v_{\text{max}} = [S]^{n_H}/(\kappa + [S]^{n_H})$, where the Hill constant $n_H > 1$ ($n_H < 1$) indicates positive (negative) cooperativity. The fitting results show that cooperativity is completely determined by the sign of B_1 : positive for $B_1 < 0$ and negative for $B_1 > 0$.

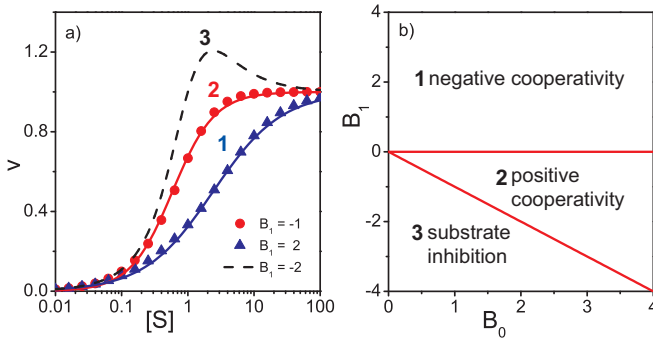


Figure 2. (Color online). (a) Three non-MM turnover rates for the single-loop model with $A_0 = B_0 = s_1 = 1$. The circles ($B_1 = -1$) and the up-triangles ($B_1 = 2$) exhibit positive and negative cooperativity, respectively. The two solid lines are the fit using the Hill equation. The dashed line ($B_1 = -2$) shows substrate inhibition behavior. (b) Phase diagram of enzyme kinetics for the single-loop model. Two lines, $B_1 = 0$ and $B_1 = -B_0$, separate three regimes of kinetics.

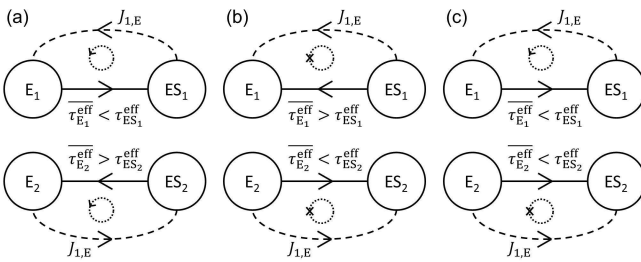


Figure 3. (a)-(c) Three cases in which a current $J_{1,E}$ circulating counter-clockwise within a two-conformation loop can be modulated by $\Delta\Delta\tau^{\text{eff}}$ (see text for details); such modulation underlies the emergence of kinetic cooperativity. In each conformational channel, a horizontal arrow proceeds from the state with the faster effective characteristic residence time (see text for details) to the state with the slower one, with $J_{1,E}$ superimposed onto this view. Note that there are also analogous cases for $J_{1,E}$ proceeding in the clockwise direction.

This result is also reflected in Eq. (6), where negative (positive) B_1 increases (decreases) the MM turnover rate $(A_0 + B_0/[S])^{-1}$. The dashed line in Fig. 2(a) shows that a largely negative $B_1 + B_0$ leads to substrate inhibition behavior. The cNESS substrate inhibition shows positive cooperativity at low substrate concentrations, and then the turnover rate decreases to a nonzero value A_0^{-1} in the substrate-saturation limit. Next, we plot the phase diagram of enzyme kinetics for the single-loop model in Fig. 2(b), which only depends on B_0 and B_1 . From this phase diagram, $\alpha = B_1/B_0$ is defined as a unique non-MM indicator for single-loop systems, with negative cooperativity for $\alpha > 0$, positive cooperativity for $-1 \leq \alpha < 0$, and substrate inhibition for $\alpha < -1$.

The direction of a conformational current alone does not predict its influence on the cooperativity, which raises the question of how currents are modulated to govern

cooperative behavior. For the two-conformation network, the simplest single-loop model, we can rewrite the non-MM term as

$$\frac{B_1}{[S] + s_1} \propto \Delta\Delta\tau^{\text{eff}} \times J_{1,E}([S]), \quad (7)$$

where $\Delta\Delta\tau^{\text{eff}} = \overline{\Delta\tau^{\text{eff}}} - \overline{\Delta\tau^{\text{eff}}}_2$, with $\overline{\Delta\tau^{\text{eff}}}_i = \tau_{E_i}^{\text{eff}} - \tau_{ES_i}^{\text{eff}}$. Here, the E_i and ES_i residence times in the decomposed representation, each independent of the non-MM term [and thus of $J_{1,E}([S])$], are given by $\tau_{E_i}^{\text{eff}}([S]) = K_{i,M}^{\text{eff}}/(k_{i,2}^{\text{eff}}[S])$ and $\tau_{ES_i}^{\text{eff}} = 1/k_{i,2}^{\text{eff}}$, respectively. Also, $\overline{\tau_{E_i}^{\text{eff}}} = \tau_{E_i}^{\text{eff}}([S] = s_1)$, where s_1 is the value of $[S]$ at which $|J_{1,E}([S])|$ is at half its maximum and thus represents a characteristic non-MM substrate concentration. Therefore, $\overline{\tau_{E_i}^{\text{eff}}}$ represents a characteristic value of $\tau_{E_i}^{\text{eff}}([S])$, with corresponding characteristic residence time gradient $\Delta\tau^{\text{eff}}_i$. Thus, $\Delta\Delta\tau^{\text{eff}}$ represents the difference in characteristic residence time gradient between the two decomposed conformational channels. Cooperativity depends upon $J_{1,E}$ modulated by $\Delta\Delta\tau^{\text{eff}}$, i.e., it is governed by the relative modulation of the current between the two decomposed chain reactions. In the two-conformation model, $J_{1,E}$ proceeds from E_i to ES_i in one conformational channel and from ES_i to E_i in the other, as illustrated in Fig. 3(a)-(c) for a counterclockwise current, which corresponds to $J_{1,E} > 0$ based upon our original definition of $J_{i,j}$. In each two-state chain reaction, enzyme turnover is accelerated (decelerated) when $J_{1,E}$ proceeds from the state with the slower (faster) effective characteristic residence time to the state with the faster (slower) one. In Fig. 3(a) [(b)], turnover is accelerated (decelerated) in both chain reactions, resulting in overall turnover acceleration (deceleration), i.e., positive cooperativity or substrate inhibition (negative cooperativity). In Fig. 3(c), turnover is accelerated in conformation 1 and decelerated in conformation 2 (the opposite [not shown] is possible as well), with the cooperativity depending upon the relative modulation of the current between the two decomposed chains. Kinetic cooperativity is thus explained as follows: when $J_{1,E}$ proceeds in the direction that, on average, corresponds to decreasing (increasing) effective characteristic residence time, positive cooperativity or substrate inhibition (negative cooperativity) occurs.

Interestingly, when the effective characteristic residence time gradient is conformation invariant, modulation of the conformational current is balanced, resulting in MM kinetics, even in the presence of circulating current (i.e., when $\Delta\Delta\tau^{\text{eff}} = 0$ and $J_{1,E} \neq 0$ for the two-conformation network). This scenario represents a unique type of nonequilibrium symmetry in multidimensional kinetic networks and is not precluded by the satisfaction of the aforementioned constraint resulting from local detailed balance. Additionally, we note that for the 2×2 model, $J_{1,E}$ vanishes under a simple conformational

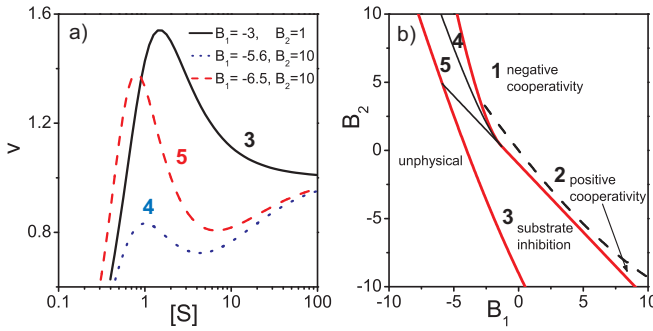


Figure 4. (Color online). Enzyme kinetics for the two-loop model with $A_0 = B_0 = s_1 = 1$ and $s_2 = 4$. (a) Three turnover rates v that are non-monotonic functions of $[S]$. Each line shows a typical type of non-MM kinetic behavior from the regime labeled by the same number in (b). (b) Phase diagram determined by two non-MM parameters B_1 and B_2 . There are five regimes of non-MM behavior (see text for details).

detailed balance condition,

$$\frac{\gamma_{1,1}}{\gamma_{1,2}} K_{1,M} = \frac{\gamma_{-1,1}}{\gamma_{-1,2}} K_{2,M}, \quad (8)$$

where $K_{i,M} = (k_{i,-1} + k_{i,2})/k_{i,1}^0$. Explicit calculations for this model are provided in the Supplemental Material [23].

Multi-loop kinetics.—For the two-loop models with two non-MM terms, the cNESS enzyme kinetics become more complicated, as illustrated in a typical phase diagram in Fig. 4(b). Except for an unphysical regime where v shows divergence and negativity, five regimes of enzyme kinetics can be characterized in the phase space composed of B_1 and B_2 . Similar to the single-loop model, when monotonically increasing to the maximum value v_{\max} in the substrate-saturation limit ($[S] \rightarrow \infty$), v can exhibit negative (Regime 1) and positive (Regime 2) cooperativity. The separation line between these two kinetic regimes, however, is hard to rigorously define. The dashed separation line in Fig. 4(b) corresponds to $n_H = 1$, where the Hill constant is empirically calculated using $n_H = \log 81 / \log([S]_{0.9v_{\max}}/[S]_{0.1v_{\max}})$ [19], and $[S]_{v_{\max}}$ is the substrate concentration for v . In Regimes 3-5, the turnover rate v is a non-monotonic function of $[S]$ [examples shown in Fig. 4(a)]. In Regime 3, with v_{\max} occurring at a finite $[S]_{v_{\max}}$, the turnover rate exhibits the same substrate inhibition behavior as the single-loop model. Alternatively, an additional local minimum of v can appear at $[S]_{v_{\min}} (> [S]_{v_{\max}})$, and v increases at high substrate concentrations instead. Two examples are shown by the dashed and dotted lines in Fig. 4(a). Based on a criterion whether the global v_{\max} appears as $[S] \rightarrow \infty$ or at the finite $[S]_{v_{\max}}$, this non-MM kinetic behavior is further divided into Regimes 4 and 5, respectively.

For the generalized N_c -loop model, cNESS enzyme kinetics can be similarly analyzed using reduced parameters from Eq. (6). In the case that all the non-MM

parameters B_n are positive (negative), the turnover rate exhibits negative cooperativity (positive cooperativity or substrate inhibition). With the coexistence of positive and negative non-MM parameters, cooperativity can be qualitatively determined by the small-[S] expansion of the turnover rate in Eq. (6), $v \sim B_0^{-1}[S] - (A_0 B_0^{-2} + \sum_{n=1}^{N_c} B_n s_n^{-1} B_0^{-1})[S]^2 + O([S]^3)$. For a largely negative $\sum_n B_n/s_n$, the positive quadratic $[S]$ term dominates in v , resulting in positive cooperativity. When this summation becomes largely positive, the cancellation between linear and nonlinear terms can slow down the increase of v with $[S]$, inducing negative cooperativity. The sign of $\sum_n B_n/s_n$ is thus a qualitative indicator of cooperativity. To investigate the substrate inhibition behavior, we expand v in the substrate-saturation limit as $v \sim A_0^{-1} - (B_0 + \sum_n B_n) A_0^{-2} [S]^{-1} + O([S]^{-2})$. For $\sum_n B_n < -B_0$, v is a decreasing function of $[S]$, and the maximum turnover rate v_{\max} must appear at a finite $[S]$. The investigation of other types of non-monotonic behavior for v needs the explicit rate form in Eq. (6).

Conclusion.—In summary, we study cNESS enzyme kinetics induced by population currents from conformational dynamics. Applying the flux balance method to a discrete $N \times M$ kinetic model, we derive a generalized Michaelis-Menten equation to predict the $[S]$ dependence of the turnover rate. Using reduced non-MM parameters, B_n in Eq. (6), our generalized MM equation provides a systematic approach to explore cNESS enzyme kinetics. Compared to the typical rate matrix approach, our flux method characterizes non-MM enzyme kinetics in a much simpler way. For example, a unique kinetic indicator $\alpha = B_1/B_0$ is defined for the single-loop model, and phase diagrams are plotted for the single- and two-loop models. Our study can be extended to other important biophysical processes following the MM mechanism, e.g., the movement of molecular motors induced by ATP binding.

This work was supported by the NSF (Grant No. CHE-0806266) and the ARO-DOD (Grant No. W911NF-09-1-04880). D. E. P. acknowledges support from the NSF Graduate Research Fellowship Program.

* Present address: Physics Department, Zhejiang University, 38 ZheDa Road, Hangzhou, Zhejiang 310027, China

† jianshu@mit.edu

- [1] L. Michaelis and M. L. Menten, *Biochem. Z.* **49**, 333 (1913).
- [2] H. Noji, R. Yasuda, M. Yoshida, and K. Kinoshita, *Nature* **386**, 299 (1997).
- [3] B. P. English, W. Min, A. M. van Oijen, K. T. Lee, G. Luo, H. Sun, B. J. Cherayil, S. C. Kou, and X. S. Xie, *Nat. Chem. Biol.* **2**, 87 (2006).
- [4] H. P. Lu, *Chem. Soc. Rev.* **43**, 1118 (2014).
- [5] C. Frieden, *Annu. Rev. Biochem.* **48**, 471 (1979).

- [6] A. Cornish-Bowden and M. L. Cárdenas, *J. Theor. Biol.* **124**, 1 (1987).
- [7] J. Cao, *Chem. Phys. Lett.* **327**, 38 (2000); S. Yang and J. Cao, *J. Phys. Chem. B* **105**, 6536 (2001).
- [8] I. V. Gopich and A. Szabo, *J. Chem. Phys.* **118**, 454 (2003).
- [9] X. Xue, F. Liu, and Z. Ou-Yang, *Phys. Rev. E: Stat., Nonlinear, Soft Matter Phys.* **74** (2006).
- [10] W. Min, I. V. Gopich, B. P. English, S. C. Kou, X. S. Xie, and A. Szabo, *J. Phys. Chem. B* **110**, 20093 (2006); W. Min, X. S. Xie, and B. Bagchi, *J. Phys. Chem. B* **112**, 454 (2008).
- [11] M. A. Lomholt, M. Urbakh, R. Metzler, and J. Klafter, *Phys. Rev. Lett.* **98** (2007).
- [12] J. Xing, *Phys. Rev. Lett.* **99** (2007).
- [13] H. Qian, *Biophys. J.* **95**, 10 (2008).
- [14] S. Chaudhury and O. A. Igoshin, *J. Phys. Chem. B* **113**, 13421 (2009).
- [15] J. Cao, *J. Phys. Chem. B* **115**, 5493 (2011).
- [16] A. B. Kolomeisky, *J. Chem. Phys.* **134**, 155101 (2011).
- [17] M. A. Ochoa, X. Zhou, P. Chen, and R. F. Loring, *J. Chem. Phys.* **135**, 174509 (2011).
- [18] A. C. Barato and U. Seifert, *J. Phys. Chem. B* **119**, 6555 (2015).
- [19] A. Fersht, *Enzyme Structure and Mechanism* (W. H. Freeman, New York, 1985).
- [20] J. Wu and J. Cao, *Adv. Chem. Phys.* **146**, 329 (2011).
- [21] J. Cao and R. J. Silbey, *J. Phys. Chem. B* **112**, 12867 (2008); T. Avila, D. E. Piephoff, and J. Cao, arXiv:1312.4909.
- [22] J. R. Moffitt and C. Bustamante, *FEBS J.* **281**, 498 (2014).
- [23] See Supplemental Material for explicit calculations for a four-state, single-loop model.